3 ARTIFICIAL EXTRACELLULAR MATRIX PROTEINS FOR RAPID WOUND HEALING

Abstract

Short RGD sequences exhibit biological activity but their responses are often not identical to that of fibronectin. Longer fibronectin fragments are difficult to purify and hence limit their use as biomaterials. Here we employ a genetic strategy to incorporate full-length fibronectin domains into artificial extracellular matrix (aECM) materials. We show that these aECM proteins promoted rapid spreading of Rat-1 fibroblasts. In particular, the aECM protein containing full-length fibronectin 9 and 10 exhibited increased $\alpha_5\beta_1$ integrin binding affinity. The aECM proteins with full-length fibronectin domains also promoted rapid wound healing of Rat-1 fibroblasts *in vitro* by supporting cell migration and proliferation; a result of increased phosphorylation of FAK and ERK.

3.1 Introduction

The discovery of the Arg-Gly-Asp (RGD) sequence (*1*) has triggered the widespread use of RGD-functionalized materials for directing cell behavior (*2*). In studies of this kind, however, cell responses on RGD surfaces are never identical to those observed on fibronectin (*3*). An obvious strategy to improve biological activity in biomaterials is to expand the RGD domain to include neighboring domains. The PHSRN domain on the 9th type III domain of fibronectin for instance, has been found to act synergistically with the RGD domain on the neighboring 10th domain (*4*). Recombinant full-length fibronectin type III domains 8 through 11 have also been shown to enhance integrin binding in cell attachment (*5-6*). However, full-length fibronectin fragments are expensive to purify in large quantities and difficult to attach to synthetic surfaces without denaturation.

Here we use a genetic strategy to fabricate biomaterials bearing full-length fibronectin domains. Functional full-length fibronectin domains 9 and 10 were incorporated within artificial extracellular matrix (aECM) proteins. Each aECM protein consists of a central full-length cell-binding domain and flanking elastin-like domains (Figure 3.1). Lysine residues were interspersed within the elastin-like sequences to allow crosslinking and fabrication of viscoelastic materials with tunable moduli (*7-8*). For simplicity, each aECM protein will be referred to by its cell binding domains (CBD).

MMASMTGGQQMGHHHHHHHDDDDKLD[(VPGIG)$_2$VPG*K*G(VPGIG)$_2$]$_6$ <u>CBD</u>[(VPGIG)$_2$VPG*K*G(VPGIG)$_2$]$_6$LE

Encoded protein (s)	CBD amino acid sequence
FN910	**FGLDSPTGIDFSDITANSFTVHWIAPRATITGYRIRH HPEHFSGRPREDRVPHSRNSITLTNLTPGTEYVVSI VALNGREESPLLIGQQSTVSDVPRDLEVVAATPTS LLISWDAPAVTVRYYRITYGETGGNSPVQEFTVPG SK̲STATISGL K̲PGVDYTITVYAVTGRGDSPASSK̲PI SINYR**
FN910m	**FGLDSPTGIDFSDITANSFTVHWIAPRATITGYRIRH HPEHFSGRPREDRVPHSRNSITLTNLTPGTEYVVSI VALNGREESPLLIGQQSTVSDVPRDLEVVAATPTS LLISWDAPAVTVRYYRITYGETGGNSPVQEFTVPG SA̲STATISGL A̲PGVDYTITVYAVTGRGDSPASSA̲PI SINYR**
FN10m	**VSDVPRDLEVVAATPTSLLISWDAPAVTVRYYRITY GETGGNSPVQEFTVPGSA̲STATISGLA̲PGVDYTITV YAVTGRGDSPASSA̲PISINYR**
RGDm	**YAVTGRGDSPASSA̲PIA**

Figure 3.1 Amino acid sequences of the aECM proteins containing full length fibronectin domains. The general sequence of the aECM proteins is shown above. Each protein contains an N-terminal T7 tag, hexahistidine tag, enterokinase cleavage site, followed by six elastin-like repeats, a cell-binding domain (CBD) and six elastin-like repeats. The amino acid sequence of the CBD used for each encoded protein is as shown. The differences between FN910 and FN910m are highlighted in yellow. The letter "m" is used to denote cell-binding domains containing lysine-to-alanine mutations.

3.2 Materials and methods

Cells, antibodies, and reagents

Dulbecco's modified eagle medium (DMEM), fetal bovine serum (FBS), penicillin/streptomycin, 0.05% Trypsin/0.25% EDTA, and PBS were obtained from Invitrogen (Carlsbad, CA). Rat-1 fibroblasts were generous gifts from the Asthagiri laboratory at Caltech. Cells were maintained in growth media containing phenol-red, 10% fetal bovine serum (FBS) and 0.1% penicillin/streptomycin through passages $9 - 25$. All experiments were performed in phenol-red-free and serum-free DMEM with 0.1% penicillin/streptomycin (SFM).

Restriction enzymes were obtained from New England Biolabs, NEB, Ipswich, MA. All ligations were performed using T4 DNA ligase (Roche Applied Science, 2.5 h, 25 ºC). DNA was isolated using QIAprep Spin Miniprep Kits (Qiagen). DNA segments encoding various cell-binding domains were purchased from Genscript (Piscataway, NJ) or Integrated DNA Technologies (IDT, San Diego, CA). Cloning was performed using *E. coli* XL10-Gold cloning strain (Stratagene) and subsequently transformed into *E. coli* strain BL21 (DE3) pLysS host (Novagen, Madison, WI) for protein expression.

Anti-phospho-FAK and anti-ERK 1/2 were purchased from Invitrogen. All other antibodies, human $\alpha_5\beta_1$ integrin, human plasma fibronectin (FN), Hoechst 33342 dye, and TMB/E substrate were obtained from Chemicon (Temecula, CA). Bovine serum albumin (BSA) was obtained from Sigma. Bis[sulfosuccinimidyl] suberate (BS^3) used for crosslinking aECM proteins was obtained from Pierce, Rockford, IL. The 5-bromo-2'-

deoxyuridine (BrdU) labeling kit was purchased from Roche Applied Science (Indianapolis, IN). Round coverslips (12mm diameter, No.1) were from Deckgläser, Germany. All Western blotting reagents were obtained from GE Healthcare (Piscataway, NJ).

Construction, expression, and purification of aECM proteins

Standard molecular biological techniques were used for DNA manipulations, bacterial growth, and electrophoresis. DNA encoding various cell-binding domains was ligated into the pET28aRW vector containing an N-terminal T7 tag, hexahistidine tag, and an enterokinase cleavage tag (*9-11*). All products were verified by restriction digestion and DNA sequencing (Laragen, Los Angeles, CA).

Expression was performed in a 10 L Bioflow 3000 fermentor (New Brunswick Scientific, Edison, NJ). Cells harboring appropriate aECM expression constructs were grown in Terrific Broth supplemented with 25 mg/ml kanamycin and 35 mg/ml chloramphenicol to an optical density at 600 nm (OD_{600}) of 6-8. Protein expression, under the control of a bacteriophage T7 promoter, was induced with the addition of 1 mM β-isopropyl thiogalactoside (IPTG, GoldBio, St Louis, MO) for 2 h. The cell pellet was harvested and resuspended in TEN buffer (10 mM Tris-HCl, 1 mM EDTA, 100 mM NaCl, pH 8) at 0.5 g/ml and purified by thermal cycling (*7, 10*). Briefly, cells were frozen at -20 ℃ and thawed with 10 μg/ml Deoxyribonuclease I, 10 μg/ml of Ribonuclease A, 50 μg/ml of Phenylmethylsulfonyl fluoride (Sigma, St Louis, MO), and 5 mM $MgCl_2$ for 3 h at 37 ℃. The solution was sonicated for 10 min using a Misonix Sonicator 3000

(Farmingdale, NY, 1/2 inch flat tip, level 7, 5 s on, 5 s off). Water was added to bring the total volume of the solution to 1.3 L, adjusted to pH 9 and stirred at 4 ºC for 2 h. The solution was centrifuged at 27915g, 1 h, 4 ºC and the supernatant was collected. The supernatant was adjusted to 1 M NaCl, warmed to 37 ºC for 1 − 2 h with shaking, and again centrifuged at 27915g, 1 h, 37 ºC. The resulting pellet was retained and re-suspended in distilled H_2O (100 mg/ml) at 4 ºC overnight. This process was repeated twice, with centrifugation spins at 39750g for better separation. The protein solution after the third cycle was dialyzed at 4 ºC for 3 days and lyophilized. Purified aECM proteins (1 mg/ml) were verified using SDS-PAGE (Figure B2). The yields obtained for each aECM protein from typical 10 L fermentations are shown in Table B1.

Preparation of spin-coated aECM films

Spin-coated aECM proteins were prepared as described previously (*11*). Glass coverslips were sonicated in a mixture of ethanol and KOH for 15 min and rinsed several times with distilled H_2O. Protein solutions were prepared by dissolving 15 mg of lyophilized of FN910 (or FN910m) in 150 µl of sterile distilled H_2O at 4 ºC for 3 − 4 h. BS^3 (2.0 mg) dissolved in 17 µl of sterile distilled H_2O was added to 150 µl of protein solution, mixed, and centrifuged to remove bubbles. The stoichiometric ratio of activated esters in BS^3 to primary amines in the aECM proteins was roughly 1:1. A 14 µl volume of BS^3-protein solution was then spin-coated on a 12 mm diameter round glass cover slip at 329g for 30 s at 4 ºC. Protein films were stored overnight at 4 ºC before use.

Cell spreading

Standard 24-well tissue culture plates were coated with aECM protein solutions (1 mg/ml) or FN (10 μg/ml) overnight at 4 ℃. Coverslips containing crosslinked aECM films were also mounted separately into the wells using sterile grease. Wells containing adsorbed proteins were rinsed with PBS and subsequently blocked with 500 μl of 0.2 wt% heat-inactivated BSA solution at room temperature for 30 min. In each well, 4 x 10^4 cells were added to 1 ml of SFM and incubated at 37 ℃ under 5% CO_2/95% air. Images of five random positions in each well were acquired every 15 min for 1.5 h. The projected cell areas for 200 cells were measured using ImageJ for each condition at various times.

$\alpha_5\beta_1$ integrin binding assay (ELISA)

In ELISA binding assays, adsorbed aECM proteins were used instead of adsorbed integrins to eliminate high levels of non-specific adsorption of aECM to polystyrene during binding. Integrin binding conditions were as reported by Altroff et al. (*5*). Briefly, FN, BSA, and various aECM proteins were dissolved in 25 mM Tris-HCl, pH 7.4, 150 mM NaCl, 1 mM $MnCl_2$, 0.1 mM $MnCl_2$, and 0.1 mM $CaCl_2$ (EB) to obtain a final concentration of 0.1 μM. Clear, flat-bottom 96-well plates (Greiner, VWR) were coated with 100 μl of various protein solutions and left overnight at 4 ℃. The plates were then washed once with EB containing 1% BSA and 0.1% Tween-20 (wash buffer), and blocked with 320 μl of EB with 5% BSA at 37 ℃ for 30 min. At the same time, $\alpha_5\beta_1$ integrins were diluted in EB with 1% BSA to various concentrations. The wells were washed twice with 200 μl of wash buffer and incubated with integrins for 2 h at 37 ℃. The wells were again washed five times with wash buffer, and 50 μl of mouse anti-$\alpha_5\beta_1$

(clone JBS5, 1:200 in EB with 1% BSA) was added to each well and incubated at room temperature for 1 h. Finally, wells were washed five times with wash buffer before adding 50 µl of goat anti-mouse-HRP (AP124P, 1:5000 in EB with 1% BSA) at room temperature for 30 min. Finally, wells were again washed five times with wash buffer and developed with 100 µl of TMB/E substrate (ES001) for 10 min at room temperature. The reaction was stopped by addition of 100 µl of 1 N H_2SO_4, and absorbance at 450 nm was read immediately using a Safire plate reader (Tecan, San Jose, CA). Assays were performed in triplicate and non-specific binding in the BSA wells for each integrin concentration was subtracted from the total binding values. The dose response data from the assays were fitted to a non-linear regression sigmoidal curve fit using Origin v.8 (OriginLab, Northampton, MA). The apparent K_D's for various aECM proteins and FN were calculated. The molecular weights of fibronectin and $\alpha_5\beta_1$ integrin were assumed to be 250 kDa and 265 kDa, respectively.

Wound healing

Wound healing was performed as described in Chapter 2 (see Figure 2.2A). Proteins were adsorbed on cleaned glass coverslips at 4 ºC for up to 1 week and air-dried before use. A thin block of PDMS was placed in the center of the glass and mounted into a 24-well plate using silicone glue. To aid cell adhesion, FN solution (500 µl, 10 µg/ml in PBS) was added to each well and incubated overnight at 4 ºC. Subsequently, all wells were aspirated before seeding Rat-1 fibroblasts in growth media. Upon reaching confluence, the growth medium was replaced with SFM, and the cells were incubated for another 24 h to arrest growth at the G0/G1 phase through contact inhibition (*12-13*).

Subsequently, the PDMS block was removed, and cells were washed twice with SFM to remove cell debris. Finally, images of several spots on the wound edge were acquired (per protein surface) every 15 min for 72 h. Images were analyzed using ImageJ v1.37. The wound area was traced manually at various time points, t, and the wound edge displacement was calculated as follows:

$$\text{Wound edge displacement } (\mu m) = \frac{\text{Wound area } (\text{t} = 0 \text{ h}) - \text{Wound area } (\text{t} = t \text{ h})}{\text{Length of wound}}.$$

Individual cell tracking

Cells at the edge of the wound sheet were tracked for 10 h from the start of wounding. Cell tracking was performed manually by tracking the centroids of each cell, using ImageJ with plug-in MTrackJ, developed by Meijering and coworkers (http://www.bigr.nl/). The average distance over time for all the tracked cells was fitted to a linear fit, and the slope was reported as the average speed. An average of 100 cells was tracked for each protein surface.

Quantification of cell proliferation using BrdU-labeling

Wounding healing experiments were performed as previously described for 24 h, after which the medium in each well was replaced with SFM containing 10 μM BrdU. Cells were incubated for another 24 h, during which cells entering S-phase could incorporate BrdU during DNA synthesis. Cells were then washed twice with pre-warmed PBS, and fixed in 70% ethanol/30% Glycine (pH 2) at -20 °C for 20 min. After washing with PBS twice, cells were incubated with 200 μl of anti-BrdU (100 μl anti-BrdU with 900 μl incubation buffer) for 30 min at 37 °C. Cells were again washed with PBS and

incubated with 1 μl Hoechst 33342 and 200 μl anti-mouse-FITC in PBS (1: 200) for 30 min at 37 °C. Finally, cells were washed twice with PBS and once with distilled H_2O before mounting with 1:1 PBS/glycerol. Cells labeled with BrdU whose locations in the cell sheet were within a distance of 350 μm of the wound edge were counted. The percent BrdU-positive cells was taken to be the number of BrdU-labeled cells as a percentage of the total Hoescht-labeled cells.

Immunoblotting

Standard 10-cm tissue culture petri dishes were coated with 3 ml of FN (10 μg/ml or 100 μg/ml in PBS), BSA (2 mg/ml in PBS), or aECM proteins (1 mg/ml in PBS) for 2 − 3 days at 4 °C. Dishes were washed twice with pre-warmed PBS, and blocked with 2 ml of heat-inactivated BSA (2 mg/ml in PBS) for 30 min at room temperature. Dishes were rinsed again twice with pre-warmed PBS. Confluent Rat-1 fibroblasts were serum-starved for 24 h (*12-13*) to arrest cell growth and reduce signaling to background. Cells were then trypsinized and held in suspension in SFM for 45 min at 37 °C to further minimize contact-mediated signaling. Subsequently, 3 x 10^4 cells/cm^2 were seeded into each well containing pre-coated proteins and allowed to adhere for 1 h at 37 °C 5% CO_2/95% air. Cells were placed on ice, washed twice with ice-cold PBS, and lysed in 300 μl of Laemmli buffer (62.5 mM Tris-Cl, pH 6.8, 20% glycerol, 10% 2-mercaptoethanol and 4% SDS). The cell lysates were collected and centrifuged at 18000*g*, room temperature for 15 min. Equal amounts of proteins were boiled for 5 min and separated on 7% or 10% SDS-PAGE gels, transferred to nitrocellulose membranes, and blocked with TBST (20 mM Tris-Cl, pH 7.6, 0.9% NaCl, 0.1% Tween-20) with 5% BSA for 1 h

at room temperature. Membranes were incubated with antibodies against FAK, phosphorylated FAK (pY397; 1:1000), ERK 1/2, and phosphorylated ERK 1/2 (Thr202/Tyr204, Thr185/Tyr187; 1:1000) in TBST with 3% BSA overnight at 4 °C. After washing with TBST, secondary antibodies (horse-radish peroxidase-conjugated anti-rabbit or anti-mouse IgG; 1:5000 in TBST) were incubated for 1 h at room temperature. Blots were washed three times for 15 min with TBST and developed according to manufacturer's instructions using the ECL Plus™ kit (GE Healthcare) and subsequently visualized by Typhoon™ Trio (GE Healthcare). Protein band intensities were measured using ImageQuant TL v7.0 and phosphorylation levels normalized to total FAK or total ERK1/2.

Statistical analysis

The statistical significance of differences was estimated by analysis of variance followed by the Tukey test. Differences were taken to be significant at $P \leq 0.05$.

3.3   Results and discussion

The amino acid sequences of the aECM proteins were designed to accommodate the large cell binding domains from fibronectin. We also mutated lysine residues to alanines in the fibronectin cell-binding domains (CBD) to eliminate any crosslinking with the lysine residues in the elastin domains, which could preclude the accessibility of the cell-recognition region for integrin binding (Figure 3.1). Large-scale expression of these constructs yielded 500 mg to 2g of purified lyophilized products per 10L of cell culture

obtained using fermentation. The purity and molecular weight of the lyophilized proteins were verified by SDS-PAGE (Figure 3.2).
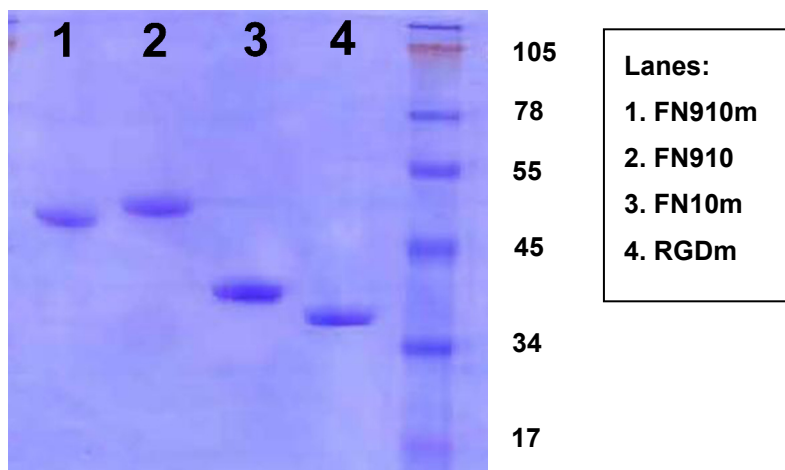

Figure 3.2 Coomassie SDS-PAGE gel of purified aECM proteins. 10 µl of each denatured protein solution (1 mg/ml in PBS pH 7.4) was loaded for each lane and run with SeeBlue Plus2 molecular weight ladder.

Fibroblasts undergo rapid migration and proliferation during wound healing to replace cell loss following an injury (*14*). Fibroblasts express both the $\alpha_5\beta_1$ and $\alpha_v\beta_3$ integrins, which are utilized for cell spreading and wound healing (*15-16*). Here, Rat-1 fibroblasts were allowed to spread on both adsorbed and cross-linked aECM films. Cells spread faster on adsorbed FN910m and FN10m compared to RGDm surfaces (Figure 3.3A). After 1.5 h, cell areas on FN910m and FN10m were comparable to those on the positive control fibronectin (FN). In contrast, the average cell area on RGDm was two-fold lower (Figure 3.3B).
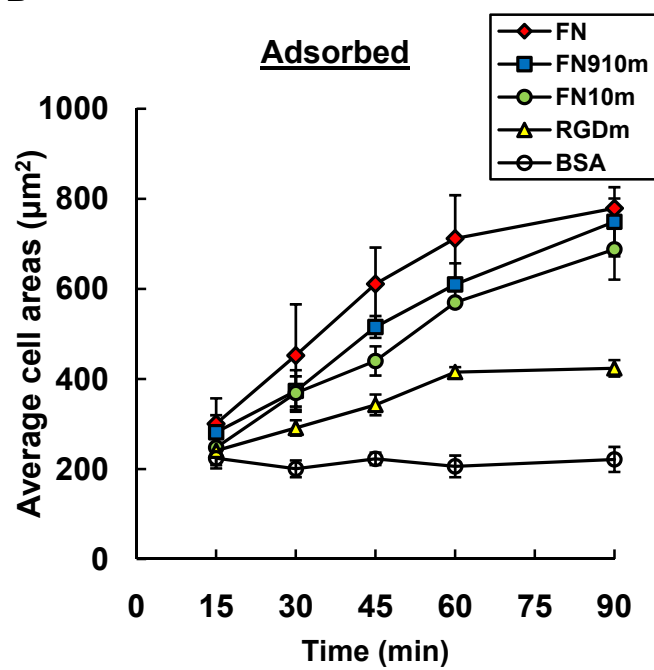
A

FN

FN910m

FN10m

RGDm

BSA

B

Adsorbed

- FN
- FN910m
- FN10m
- RGDm
- BSA
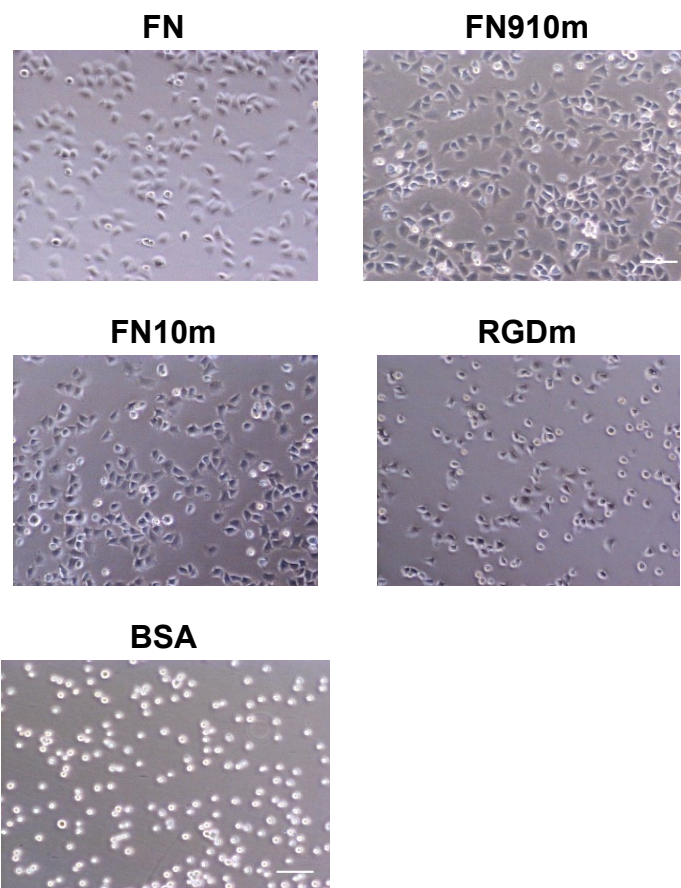
Figure 3.3 Time course of cell spreading of Rat-1 fibroblasts on adsorbed protein surfaces.
(**A**) Phase contrast images of spreading of Rat-1 fibroblasts on various adsorbed protein surfaces after 1.5 h. (**B**) The average projected cell areas for the adsorbed protein surfaces at each time point. Data represent means ± SEM from three independent experiments. Scale bar represents 100 µm.

A similar trend was also observed on cross-linked aECM films (Figure 3.4A). There were also no differences in cell spreading behavior on cross-linked FN910 and FN910m, suggesting that the lysine-to-alanine mutations had no effect on the overall biological activity of the aECM proteins (Figure 3.4B).

A

B
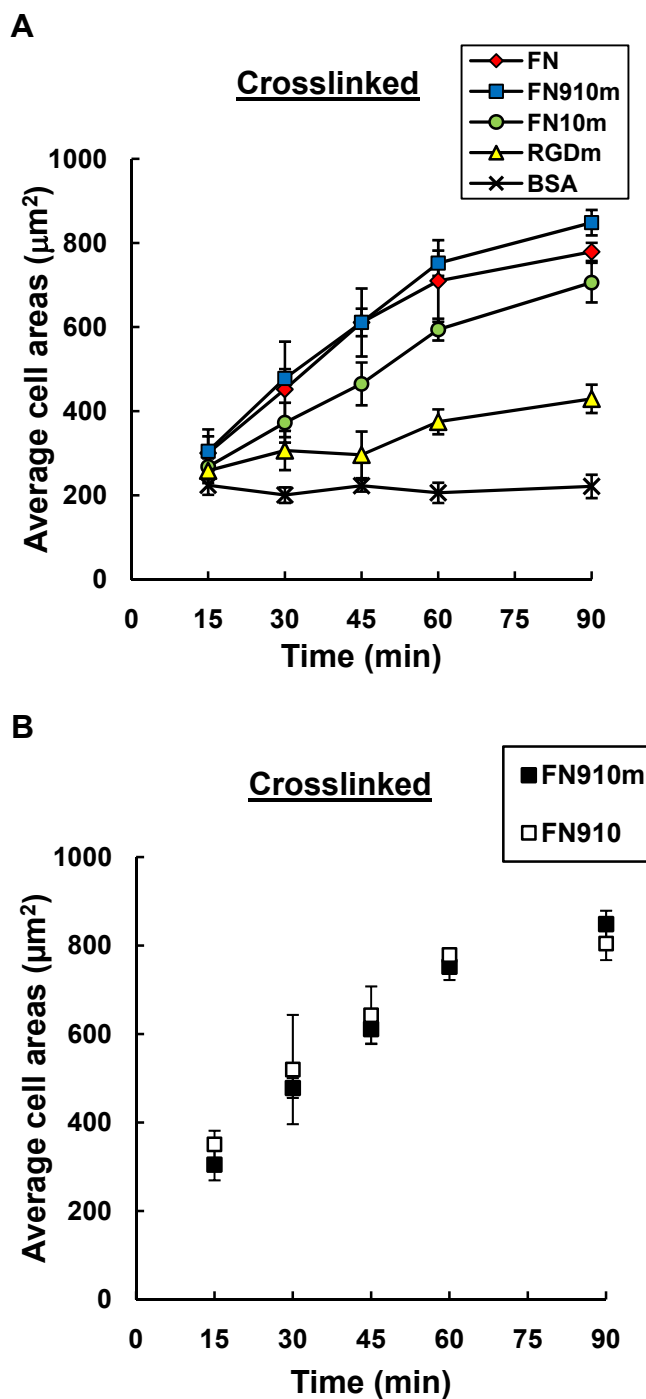
Figure 3.4 Time course of cell spreading for crosslinked aECM protein surfaces. (**A**) Cell spreading on spin-coated crosslinked FN910m, FN10m, and RGDm compared to adsorbed FN and BSA control surfaces. (**B**) Rat-1 cell spreading on spin-coated crosslinked FN910 and FN910m

Fibroblasts have been shown to spread faster on surfaces that promote specific $\alpha_5\beta_1$ integrin binding (*17*). To see if aECM proteins containing full-length cell-binding domains promoted increased integrin binding, we used a modified solid-phase integrin binding assay (ELISA). Indeed, we found a 10-fold enhancement in $\alpha_5\beta_1$ integrin binding affinity for FN910m (17.2 nM), compared to FN10m (109 nM) and RGDm (100 nM). Under the same conditions, the $\alpha_5\beta_1$ binding affinity for FN was 6.2 nM (Figure 3.5). The values for FN910m were higher than reported K_D values of 2 – 4 nM (*6, 18-19*), but were most likely due to the way the integrins are presented (i.e., immobilized integrins versus soluble integrins). The increase in $\alpha_5\beta_1$ integrin binding affinity also confirmed the synergistic effect of PHSRN (*6, 18*), suggesting that the full-length FN910 domains within the aECM proteins are indeed functional.

We did not see any significant differences in $\alpha_5\beta_1$ integrin binding affinities for FN10m and RGDm (Figure 3.5). However, FN10m promoted faster cell spreading than RGDm (Figure 3.3B and Figure 3.4A). A possible explanation for the increase in cell spreading rates on FN10m could be due to increased accessibility of the RGD loop with the increased structural stability of the full-length fibronectin 10 domain. Another possibility could be that FN10m promotes an increased binding affinity to the vitronectin receptor ($\alpha_v\beta_3$) integrin (*20-21*).
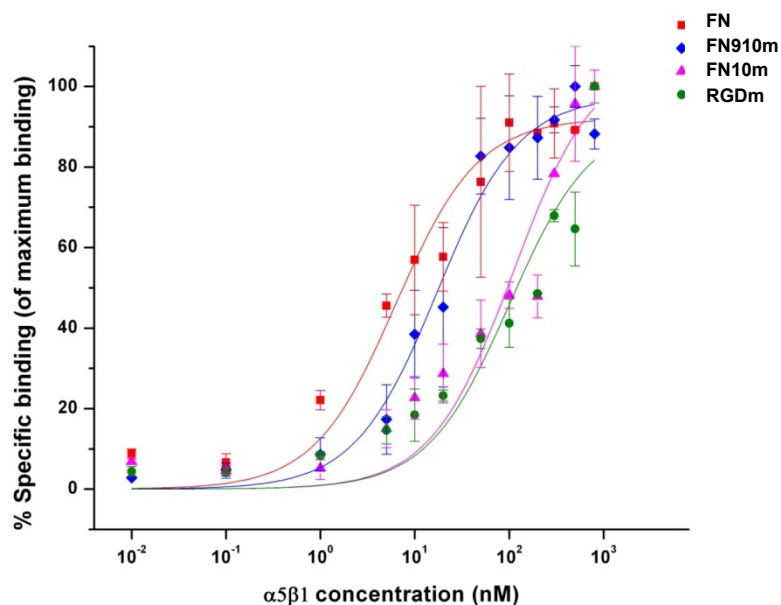
	FN	FN910m	FN10m	RGDm
Apparent K_D	6.3 nM	17.2 nM	109 nM	100 nM

Figure 3.5 Binding of $\alpha_5\beta_1$ integrin to fibronectin and aECM proteins by ELISA. Individual dose-response curves for various surfaces were corrected for non-specific binding in the BSA wells. Results are normalized and expressed as percentages of maximum binding activity. The apparent K_D's were derived by fitting the data to a non-linear regression sigmoidal curve fit for each surface.

Given the faster cell spreading on the aECM proteins with full-length cell-binding domains, we next examined the ability of these proteins to promote wound healing using the wound healing assay developed in Chapter 2. Collective migration was observed on all adsorbed protein surfaces except on uncoated glass and BSA surfaces. Cells at the wound edge developed a polarized morphology after 2 h, extending their lamellipodia in

the direction of the wound (*22*). Cells consistently moved in the direction of the wound, and proliferation was observed after 24 h at the wound edge.
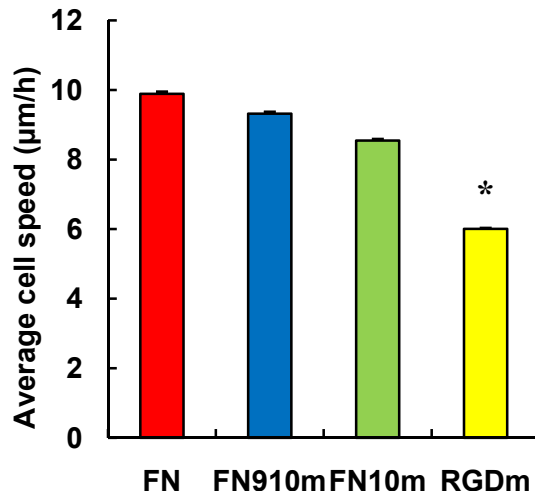
Figure 3.6A shows the wound edge displacement on various adsorbed protein surfaces over 72 h. In the first 24 h, cell sheets migrated with similar rates on FN, FN910m and FN10m surfaces. There were no significant differences between FN910m and FN10m; both surfaces supported faster migration than RGDm. Individual cells at the migrating wound edge were tracked for 10 h from the start of wounding. The average cell speeds are shown in Figure 3.6B. Cell speeds on FN910m (9.2 ± 0.8 μm/h) and FN10m (8.3 ± 0.6 μm/h) were comparable to that on FN (9.4 ± 0.8 μm/h). On the other hand, cells migrated significantly slower on RGDm (5.9 ± 0.4 μm/h; $P < 0.05$), accounting for the overall slower wound closure on RGDm.

The general wound healing behavior on aECM proteins with full-length fibronectin domains was also different than on FN after 24 h (Figure 3.6A). These differences could be accounted for by increased proliferation on FN910m and FN10m. Wounded Rat-1 monolayers were first allowed to migrate for 24 h in serum-free media and subsequently incubated with 50 μM of bromodeoxyuridine (BrdU) for another 24 h (t = 24 to 48 h). The number of BrdU-labeled cells is reported as a percentage of total Hoechst-positive cells in Figure 3.6C. The percentages of BrdU-labeled cells on the aECM proteins surfaces were significantly higher than that on FN, which would explain the slower wound healing behavior on FN at t > 24 h (Figure 3.6A).
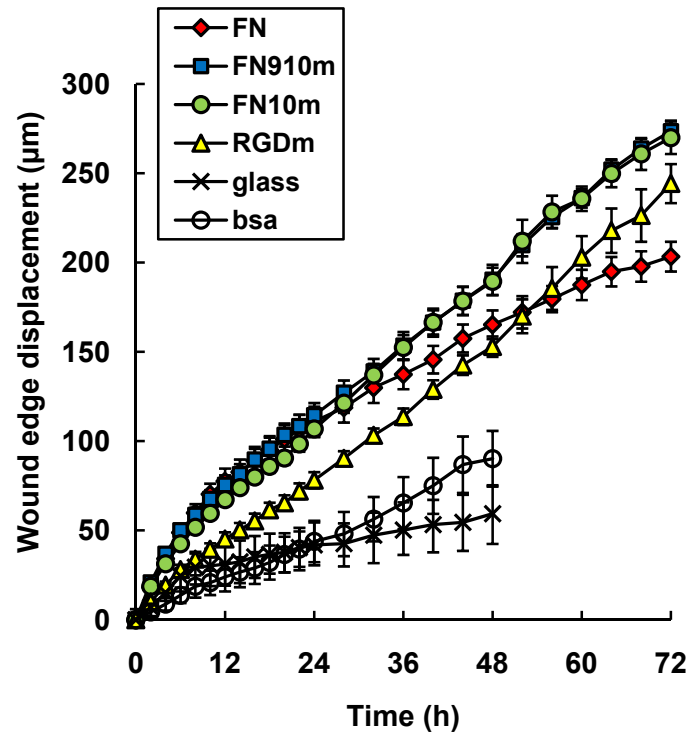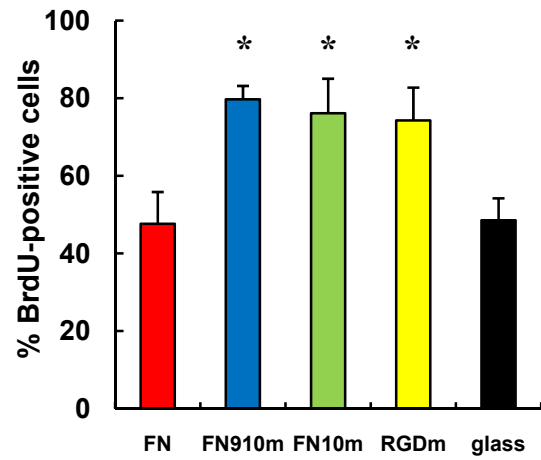
Figure 3.6 Quantification of wound healing behavior on adsorbed protein surfaces. (**A**) Rat-1 monolayers were wounded and allowed to migrate over various protein surfaces. The displacement of the wound edge as a function of time is shown. (**B**) Average speeds of cells migrating on various surfaces from t = 0 to 10 h. Individual cells in the first row of the wound edge were tracked for 10 h post wounding. Cell speeds are slopes from linear fit of distance over time data. Error bars are standard errors from fit. (**C**) The percentage of BrdU-positive cells for the period of t = 24 to 48 h (wounding; t = 0 h). The number of BrdU-labeled cells located in the cell sheet within 350 μm from the wound edge was represented as a percentage of the total number of Hoechst-positive cells in the same region. Data are means ± SEM from five independent experiments for each surface. *, significant difference from FN surface (P < 0.05).

The difference in wound healing behavior on FN and aECM proteins is likely due to differences in cell signaling. To dissect these differences, we examined the key cell signaling pathways involved in wound healing. The focal adhesion kinase (FAK) is up-regulated during integrin-mediated signaling in cell migration (*23*), while the extracellular signal-regulated kinase (ERK) pathway is activated during cell proliferation (*24-25*). Figure 3.7 shows amounts of phosphorylated FAK and ERK represented as ratios of total FAK and ERK. We found high levels of P-FAK on FN, FN910m and FN10m, accounting for faster cell speeds measured on these surfaces (Figure 3.7A and Figure 3.6B).

Consistent with the BrdU data (Figure 3.6C), high levels of P-ERK were also found on all aECM protein surfaces (Figure 3.7B). The P-ERK/ ERK ratio was significantly lower on FN (P < 0.05), suggesting that the lower proliferation rate observed

on FN was due to low levels of ERK phosphorylation. To ensure that these observations were not due to low FN concentrations, we repeated these experiments with ten-fold higher FN concentrations (i.e., 100 µg/ml). As expected, the degree of phosphorylation for both FAK and ERK was unchanged.
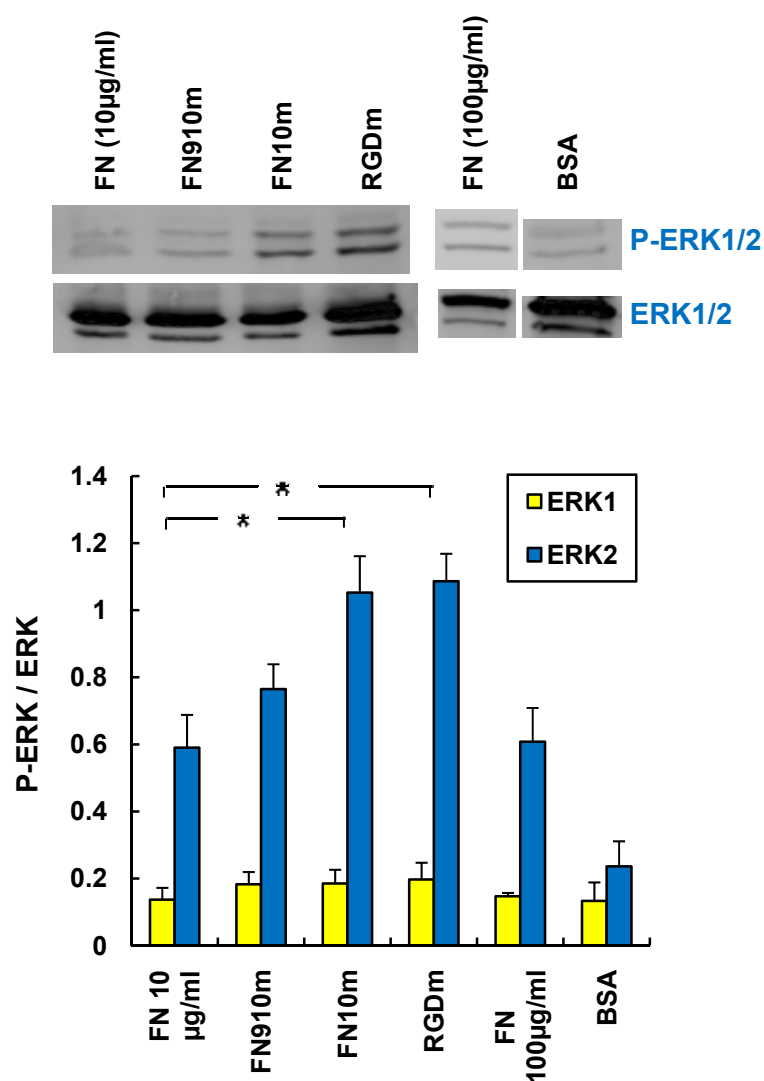
A
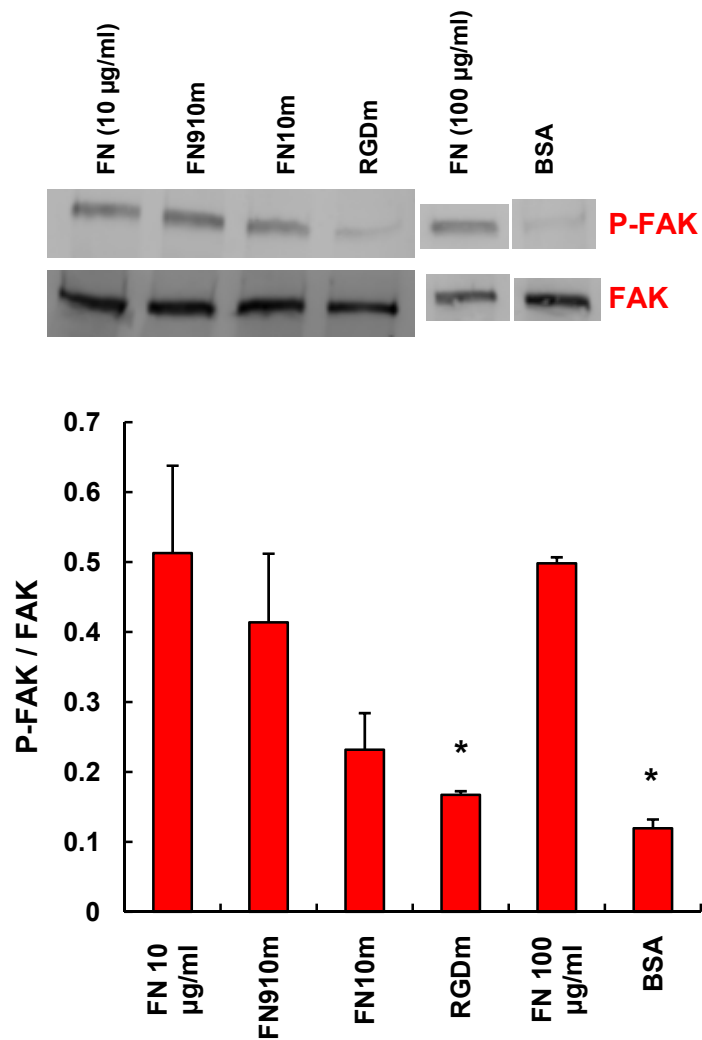
B

Figure 3.7 Determination of FAK and ERK phosphorylation in Rat-1 fibroblasts on adsorbed protein surfaces. (**A, B**) Rat-1 fibroblast cell sheets were serum-starved for 24 h, held in suspension in SFM for 45 min and allowed to attach onto protein-coated 10-cm petri dishes at 3.8×10^4 cells/cm^2. The cell lysates were analyzed by Western blotting with anti-FAK, anti-phosphoFAK (pY397), anti-phosphoERK1/2(p42/p44) and anti-total ERK1/2, antibodies. Band intensities were normalized to total-FAK or total-ERK bands. Reported data are means ± s.d. for three independent experiments. *, significantly different from FN surface ($P < 0.05$)

3.4   Conclusions

In this work, we developed functional biomaterials incorporating full-length cell-binding domains. We showed that the artificial extracellular matrix proteins containing full-length fibronectin domains promoted rapid cell spreading of Rat-1 fibroblasts. The aECM protein containing full length fibronectin 9 and 10 was shown to bind the $\alpha_5\beta_1$ integrin with higher affinity, confirming the synergistic effect between the PHSRN and RGD cell binding domains. The aECM proteins containing full-length fibronectin domains 9 and 10 also promoted rapid wound healing *in vitro* by supporting cell migration and proliferation. The increase in cell migration speeds and proliferation observed on these surfaces was due to increased phosphorylation of FAK and ERK.

3.5   Acknowledgements

3.6   References

1.   E. Ruoslahti, M. D. Pierschbacher, *Science* **238**, 491 (1987).

2.   U. Hersel, C. Dahmen, H. Kessler, *Biomaterials* **24**, 4385 (2003).

3. H. B. Streeter, D. A. Rees, *J. Cell Biol.* **105**, 507 (1987).

4. S. Aota, M. Nomizu, K. M. Yamada, *J. Biol. Chem.* **269**, 24756 (1994).

5. H. Altroff et al., *J. Biol. Chem.* **276**, 38885 (2001).

6. H. Altroff, L. Choulier, H. J. Mardon, *J. Biol. Chem.* **278**, 491 (2003).

7. P. J. Nowatzki, D. A. Tirrell, *Biomaterials* **25**, 1261 (2003).

8. P. J. Nowatzki, C. Franck, S. A. Maskarinec, G. Ravichandran, D. A. Tirrell, *Macromolecules* **41**, 1839 (2008).

9. S. C. Heilshorn, K. A. Di Zio, E. R. Welsh, D. A. Tirrell, *Biomaterials* **24**, 4245 (2003).

10. J. C. Liu, S. C. Heilshorn, D. A. Tirrell, *Biomacromolecules* **5**, 497 (2003).

11. J. C. Liu, D. A. Tirrell, *Biomacromolecules* **9**, 2984 (2008).

12. C. Schorl, J. M. Sedivy, *Methods* **41**, 143 (2007).

13. W. A. Kues et al., *Biol. Reprod.* **62**, 412 (2000).

14. J. Gailit, R. A. F. Clark, *N. Engl. J. Med.* **2**, 738 (1999).

15. R. A. F. Clark, J. Q. An, D. Greiling, A. Khan, J. E. Schwarzbauer, *J. Invest. Dermatol.* **121**, 695 (2003).

16. J. Gailit, R. A. F. Clark, *J. Invest. Dermatol.* **106**, 102 (1996).

17. S. P. Massia, J. A. Hubbell, *J. Biomed. Mater. Res. A* **56**, 390 (2001).

18. R. P. Grant, C. Spitzfaden, H. Altroff, I. D. Campbell, *J. Biol. Chem.* **272**, 6159 (1997).

19. A. P. Mould et al., *J. Biol. Chem.* **272**, 17283 (1997).

20. T. A. Petrie, J. R. Capadona, C. D. Reyes, A. J. Garcia, *Biomaterials* **27**, 5459 (2006).

21. Y. Mao, J. E. Schwarzbauer, *Cell Comm. Adhesion* **13**, 267 (2006).

22. C. D. Nobes, A. Hall, *J. Cell Biol.* **144**, 1235 (1999).

23. D. J. Sieg et al., *Nat. Cell Biol.* **2**, 249 (2000).

24. L. Barberis et al., *J. Biol. Chem.* **275**, 36532 (2000).

25.   H. R. Reiske, J. H. Zhao, D. C. Han, L. Ann Cooper, J. L. Guan, *FEBS Letters* **486**, 275 (2000).